HHS Public Access

Author manuscript

Biochim Biophys Acta. Author manuscript; available in PMC 2017 August 04.

Published in final edited form as:

Biochim Biophys Acta. 2016 September ; 1860(9): 1877–1883. doi:10.1016/j.bbagen.2016.05.039.

Monitoring drug induced apoptosis and treatment sensitivity in non-small cell lung carcinoma using dielectrophoresis

Rajeshwari Taruvai Kalyana Kumar[a], **Shanshan Liu**[b], **John D. Minna**[b], and **Shalini Prasad**[a,*]

[a]Department of Bioengineering, University of Texas at Dallas, Richardson, TX 75080, United States

[b]Hamon Center for Therapeutic Oncology Research, University of Texas Southwestern Medical Center, Dallas, TX 75390, United States

Abstract

Non-invasive real time methods for characterizing biomolecular events that contribute towards apoptotic kinetics would be of significant importance in the field of cancer biology. Effective drug-induced apoptosis is an important factor for establishing the relationship between cancer genetics and treatment sensitivity. The objective of this study was to develop a non-invasive technique to characterize cancer cells that are undergoing drug-induced apoptosis. We used dielectrophoresis to determine apoptotic cells as early as 2 h post drug treatment as compared to 24 h with standard flow cytometry method using non-small cell lung cancer (NSCLC) adenocarcinoma cell line (HCC1833) as a study model. Our studies have shown significant differences in apoptotic cells by chromatin condensation, formation of apoptotic bodies and exposure of phosphatidylserine (PS) on the extracellular surface when the cells where treated with a potent Bcl-2 family inhibitor drug (ABT-263). Time lapse dielectrophoretic studies were performed over 24 h period after exposure to ABT-263 at clinically relevant concentrations. The dielectrophoretic studies were compared to Annexin-V FITC flow assay for the detection of PS in mid-stage apoptosis using flow cytometry. As a result of physical and biochemical changes, inherent dielectric properties of cells undergoing varying stages of apoptosis showed amplified changes in their cytoplasmic and membrane capacitance. In addition, zeta potential of these fixed isolated cells was measured to obtain direct correlation to biomolecular events.

Keywords

Non invasive electrokinetics; Apoptosis monitoring; Dielectrophoresis; Non-small cell lung cancer

1. Introduction

Apoptosis or programmed cell death is an essential process for embryogenesis, mechanisms of cell homeostasis, tissue integrity, and tumor regression [1]. Apoptosis usually occurs during cell development and aging so as to maintain cell populations in tissues. It also

*Corresponding author. shalini.prasad@utdallas.edu (S. Prasad).

Transparency Document

The transparency document associated with this article can be found, in online version.

activates as a defense mechanism module as in the case of immune reactions or when cells are introduced to disease/noxious agents [1,2]. Although there are wide variety of stimuli and conditions (physiological and pathological) that can trigger apoptosis, it is an important and distinctive mode/process to study cell behavior [3]. Identifying cells undergoing apoptosis is critical for developing new cancer targeted therapeutic agents [4]. Apoptosis pathway is initiated when a family of proteins known as caspases, and perhaps other proteases, are activated in the early stages of apoptosis [5]. These proteins in turn cleave key proteins that are biochemically active to keep the cytoskeleton and nucleus stable. As a result there are two main categories of proteins that function in the formation and dissolution of membrane asymmetry that happen during apoptosis, flippases and floppases. These are the two protein categories that are involved in creating membrane asymmetry that catalyze the movement of specific phospholipid species from the extracellular leaflet of the cell membrane to the cytosolic leaflet and vice-versa [6]. This can be witnessed as mid-stage apoptosis, where variety of internal protein biomarkers become expressed on the outside of the cell's lipid bilayer membrane [2]. This results in DNA cleavage at the linker regions between oligonucleosomes. The consequence of these biochemical events cause a change in the morphology of cells as well as extreme damage leading to cellular dysfunction also known as late stage apoptosis [7]. In the study of apoptosis, focus has largely been placed on developing assays or methods that can detect different stages of apoptosis such as Annexin V assay, propidium iodide (PI) assay and many others [8,9]. These assays use fluorescent marker tags that bind to various protein biomarkers expressed during each stage of apoptosis as discussed above. For example, Annexin V assay is associated with monitoring changes in the expression of phosphatidylserine at the cell's outer lipid bilayer membrane while propidium iodide, a fluorochrome, binds to degraded DNA present at the later stages of apoptotic cells which consequently stains the nucleus of non-viable cells.

The aforementioned assays are flow cytometry based and hence require accurate identification of acquisition parameters. This challenges the discrimination of true apoptotic nuclei from nuclear debri [10]. Although flow cytometry appears to offer a number of advantages, it provides relatively little insight on events that occur within the cells prior to detection of apoptosis. Previously identified is the buildup of ions/charges that occurs on the surface as well as within the cell post apoptotic induction by a drug [11]. It has also been identified that the effective dielectric property of the cell changes as a consequence of this charge imbalance. When these changes are measured in real time, they offer a useful and important method to observe and quantitate early biophysical changes that occur during apoptosis [12]. These changes in ionic concentration within and outside of the cell can be monitored and studied using electrokinetic methods. Dielectrophoresis (DEP) and electrorotation (ROT) are commonly used electrokinetic methods that separate and characterize cells based on their inherent dielectric properties, such as cell membrane permittivity (ε_{mem}), cytoplasmic conductivity (σ_{cyto}) and specific membrane capacitance (C_{mem}) [13,14]. These factors are directly dependent on the charge buildup and polarizability of cells under applied electric fields. The apoptotic cycle of a cell from both morphological and electrical alterations are illustrated in Fig. 1.

Electrokinetic methods are widely used to separate target cells from a heterogeneous sample population, manipulate cells towards self-assembly, and characterize them based on their

biochemical signatures in a label-free manner [13]. DEP, is the most widely used electrokinetic technique that uses directional motion of particles or cells in nonuniform time variant electric fields [15]. DEP has a variety of applications that involve numerous types of organic and inorganic particles that enable us to observe their responses to various electrical stimuli, measured as function of frequency of the applied electric fields [16]. In cell biology, DEP can provide a quantitative measure of cellular properties and in our previous studies it was used to investigate cell separation and characterization along with identifying suitable buffers that could be used for cell studies [17]. DEP has been employed in a variety of cancer cell studies and is often used to characterizing cell sub populations [18]. We have also incorporated DEP as a tool to study and characterize dielectric properties of cancer cells at different stages of cell cycle.

In this study, we demonstrate that DEP can be used to characterize the apoptotic behavior of NSCLC HCC1833 cells a line with neuroendocrine features representing ~10% of pathologically diagnosed NSCLCs that is known to undergo dramatic apoptosis following exposure to Bcl-2 antagonists [19]. We began with the hypothesis that ionic concentration of cells will vary post treatment with apoptosis inducing drugs, and consequently, significant differences in the cellular apoptotic cycle can be observed using dielectrophoresis. We have evaluated this hypothesis by using Navitoclax, a Bcl-2 family inhibitor that potentiates apoptosis to assess whether apoptotic induction can be detected at multi-time points (2, 6, 10 and 24 h) following treatment using DEP. We have also used two standard bench-top techniques (Annexin V-FITC assay and Propidium Iodide assay) to compare and validate our DEP results for different stages of apoptosis. The DEP data revealed significant differences in ionic content of NSCLCs 2, 6, 10 and 24 h after treatment with Navitoclax. Additionally, late stage apoptosis was observed with significant changes in the cells' dielectric properties as early as 2 h after the treatment. In addition, we also performed a time lapse studies with time points post 6, 10 and 24 h after treatment to observe increase in the population of necrotic cells and validated using benchtop techniques. The early stages of apoptosis was not detectable using Annexin V assay and PI fluorescence was observed with confidence after 10 h of treatment. This indicates that DEP, can potentially be used in conjunction with these standard benchtop methods to enhance the temporal resolution of system efficiency.

2. Materials and methods

2.1. Materials

RPMI 1640, and phosphate buffered saline (PBS) were purchased from Sigma Aldrich. Fetal bovine serum (FBS) was purchased from ATCC. Trypsin-EDTA, Navitoclax (ABT-263), and Annexin V-FITC were purchased from Fisher Scientific. Propidium iodide was purchased from Abcam. Polydimethylsiloxane (PDMS) was purchased from Dow Corning. All chemicals and reagents were of analytical grade and used without further processing.

2.2. Cell culture and apoptosis induction

The HCC1833 neuroendocrine NSCLC (NE-NSCLC) line was obtained from the Hamon Cancer Center Collection (University of Texas Southwestern Medical Center), maintained in RPMI-1640 medium supplemented with 5% FBS without antibiotics at 37 °C in a humid

atmosphere containing 5% CO_2 and 95% air. Cells lines were DNA-fingerprinted using Powerplex 1.2 kit (Promega), and mycoplasma was tested using an e-Myco kit (Boca Scientific). Cells lines were grown up to 70% confluence before splitting. ABT-263, a potent small molecule inhibitor of Bcl-2 family, was initially dissolved in DMSO and warmed at 37 °C for 10 min in an ultrasonic water bath. The stock solution was then diluted serially to different concentrations till a final concentration of 1 μM. The drug with final concentration of 1 μM was introduced to the cell culture after the cells were adhered to the culture plate (~4.5 h after plating). Each culture plate (for varying time points) was maintained at 2 to 3 million (10^6) cells/mL cell density and was treated 1 μM of ABT-263, clinically relevant concentration that is probably saturating for Bcl-2 family binding.

2.3. DEP chip and experimental design

The DEP chips used for this study consist of standard gold interdigitated electrode design that was lithographically fabricated along with polydimethylsiloxane microfluidic sample holder assembled on a microscopic glass slide. Fabricated microelectrodes were of 250 μm width and 1000 μm in length. Series of these microelectrodes weredesigned horizontally (working electrodes) and orthogonally (reference electrodes) placed at equidistance of 250 μm from each other. Microfluidic channel was designed with height of 250 μm and width of 500 μm. Electrical voltage input signal was applied using function generator (Tektronix) resulting in the generation of nonuniform electric fields. HCC1833 cells were centrifuged at room temperature at 200 ×*g* for 5 min. The pellet was washed and resuspended in formulated isotonic medium. The medium was prepared using sucrose (8.5 *w*/*v*), dextrose (0.3 *w*/*v*) and equivalent measure of sodium chloride to maintain isotonicity in deionized water as described [17, 20]. The medium was adjusted to 50 mS/m using PBS and RPMI and the final conductivity was measured and verified using Accumet conductivity meter. The final cell density for DEP studies was counted using a hemocytometer and measured to be 2–2.5 × 10^6 cells/mL. Cellular responses to the applied electric fields were studied through time lapse imaging using inverted optical microscope and CCD camera (Leica Microsystems). Input voltage of 8 V_{pp} was applied throughout the DEP experiments which was identified based on an initial study involving a spectrum of input voltages ranging from 1 V peak to peak (V_{pp}) to 10 V_{pp}. The biophysical properties of the cells, after the incubation with ABT-263, were determined by fitting the measurement dielectrophoretic spectra obtained through DEP model [21] to match the data obtained by the DEP experiments as a function of input signal frequency. These steps were kept consistent and repeated for both treated and untreated cell population subset. For each incubation time period, post-addition of drug, DEP experiments were repeated 5 times, using different cell populations at a time in order to reduce the effect of variation in cell number. The data represented as mean ± SD and statistical analysis was performed using GraphPad (San Diego, CA). One-way ANOVA was used with *t*-test to compare the data groups with control, and differences were considered significant if *P* values were <0.05. All physical characteristics of cells were observed and measured from the time lapse videos taken.

2.4. Flow cytometry assay

Two major types of assay (Annexin-V and propidium iodide) has been widely used to detect apoptotic cells from mid- to late-stages. They are indicated by (1) cytomorphological

alterations, and (2) DNA fragmentation. Some proteins such as caspases, PS are expressed only transiently.

2.4.1. Annexin V-FITC assay—Externalization of phosphatidylserine (PS) residues on the outer plasma membrane of apoptotic cells can be deduced via Annexin V assay. The critical aspect of the Annexin-V assay is ensuring proper controls to stain only the cells with membrane integrity of the PS positive cells. HCC1833 cells were cultured to reach 90% confluence for flow cytometry studies. The cells were exposed to 500 nM concentration of ABT-263 after they were harvested and suspended in binding buffer. At time points 60 and 90 min, Annexin V assay was performed by staining with Annexin V-FITC for 15 min at 4 °C in dark. Then stained cells were suspended in binding buffer and was processed through flow cytometer (BD Accuri C6) and data was processed using the instrument's software.

2.4.2. Propidium iodide (PI) assay—PI flow assay has been used to study and detect cells at late-stage apoptosis, where PI dye stains the nucleus of the cell. PI assay was performed simultaneously with Annexin V assay to distinguish between viable, necrotic and apoptotic cells. For both flow assays cell density of 5×10^5 cells were used respectively. The method was carried out according to manufacturer's instructions and analysis was performed using the flow cytometer. The detection for Annexin V was made using FITC detector at 530 nm and a PI detector at 600 nm PI filter. Adjustments were made to decrease signal overlap between the measurements.

2.5. Zeta potential measurements

Zeta potential for sample population at each time point (t = 0, 2, 6, 10 and 24 h) post treatment were recorded in a suspension (~0.5×10^6 cells/mL) using the electrophoretic light scattering technique on a Zetasizer Nano ZS analyzer (Malvern Instruments, TX). The measurements were performed using a U-shaped cuvette with gold plated electrodes at 25 °C and neutral pH salt buffer containing no chlorine ions. Buffer conductivity was maintained at 16 ± 0.5 mS/cm. Sample viscosity was set to 1 cP with dielectric constant as 79 and refractive index of 1.338. The results obtained was an average from n = 3 replicates with standard deviation calculated for the distribution window. The results were processed using the dispersion technology software provided with the instrument (Malvern Instruments). System's equilibration time was maintained at 120 s to reduce system noise between each measurement.

3. Results and discussion

3.1. Effect of ABT-263 on NE-NSCLCs

Previously Augustyn et al., demonstrated the effect of Bcl-2 family inhibitor, ABT-263 to reduce HCC1833 cell viability through induction of apoptosis [19]. B-cell lymphoma 2 (Bcl-2) is an important anti-apoptotic protein and classified as an oncogene [22]. Treatment of NE-NSCLC cell line HCC1833 with ABT-263 resulted in induction of cell death with various concentrations of DMSO used as a control. During apoptosis poly(ADP-ribose) polymerase (PARP) is cleaved by caspase-3 and possibly by other caspases, into a smaller

molecular weight fragment, commonly known as p85 [23]. ABT-263 treatment of HCC1833 cells induces dose-dependent (50 nM, 100 nM and 500 nM respectively) cleavage of PARP and Caspase 3 after 12 h while no cleavage of PARP and Caspase-3 proteins were observed with DMSO treatments. Results from this study indicates 24 h post ABT-263 treatment of HCC1833 resulted in induction of cells in sub-G1 phase, indicating DNA flocculation during the apoptotic cascade. Critical drug concentration of 500 nM of ABT-263 demonstrates significant differences (n = 3 for each group with $^{*}P < 0.05$; $^{**}P < 0.01$; $^{***}P < 0.005$) in percentage of cells observing hypodiploid Sub-G1 phase. Induction of cell death observed was 10 to 30-fold greater ($^{***}P < 0.001$; n = 3 per treatment) than that seen in DMSO control samples [19]. Furthermore, mouse xenograft studies showed significant decrease reduction in tumor volume, size and weight, as reported in [19]. These experimental results help design the dielectrophoretic experiments. Clinically relevant concentration (1 μM) of ABT-263, greater than critical concentration (500 nM) was used in this study. In addition to electrokinetic analysis, flow cytometry assay and zeta potential measurements were performed to observe the apoptotic pathway.

3.2. Flow cytometry analysis

The effect of ABT-263 on HCC1833 cell line was analyzed by double staining with Annexin V-FITC and PI. Representative data from flow cytometry analysis is shown in Fig. 2. In this work, subsequent detection of cellular changes using flow cytometry was observed and analyzed at time points t = 2, 6, 10 and 24 h with DMSO treatment used as a control. The assay used Annexin V-FITC conjugate and propidium iodide dye to detect the exposure of PS exposure and simultaneously distinguish viable or apoptotic cells. The transfer of PS to the outside of the cell membrane allowed for the transfer of fluorescent dyes into the cell in a unidirectional manner [24,25]. Although significant numbers of HCC1833 cells had their cell membrane intact even during late phase of cell disintegration phase, microscopic analysis shows clear evidence of nuclear fragmentation. This effect was clearly observed using propidium iodide dye (orange-red color), which became internalized only in cells whose membranes have become permeable.

These results demonstrate that at incubation time points 2 and 6 h apoptotic cells were not detected. However, at incubation time t = 10 h, slight increase in percentage of apoptotic cells was observed. Percentage of apoptotic cells increased to approximately 22% after 24 h incubation with ABT-263. This study correlates to the preliminary finding reported by Augustyn et al., which indicates 30-fold increase in cell population demonstrating cells in Sub-G1 in cell cycle distribution [19]. Control population of cells treated with DMSO did not significantly differ in cell viability data over the same period of time with ~99% of HCC1833 cells remaining viable over 24 h. Standard deviation for all data points was less than 2% (n = 3 replicates were performed for each experimental group).

Annexin V and PI double-stained cells collected from the flow cytometry assay at the individual incubation time points (t = 2, 6, 10 and 24 h), was observed for distinguishing apoptotic cell subtypes using confocal microscopy. Microscopic evidence of apoptosis induction in HCC1833 cells is shown in Fig. 3. Early apoptosis cell population were marked with Annexin V-FITC [PI(−)/AnV(+)] and late apoptosis was indicated by double staining of

PI and Annexin V-FITC [PI(+)/ AnV(+)] along with control population ([PI(−)/AnV(−); [PI(+)/ AnV(−)]). A significant increase in the PI staining of apoptotic cells was observed at time t = 10 and 24 h. Microscopic image confirm the induction of apoptosis in cells post 10 and 24 h, indicating the transfer of PS to the outside of the cell membrane during apoptosis.

3.3. Zeta potential studies

Our goal was to understand the electrical behavior of cells and correlate these data to cellular changes which occur when cells undergo apoptosis. During apoptosis, rearrangement of charges and ions inside and outside cell membrane [20]. The cell surface charge is a key biophysical parameter that depends on the composition of cytoplasmic membrane and the physiological conditions of cells. The cell surface charge during morphological and biochemical changes can be monitored using zeta potential (ζ), which characterizes the electrical double layer potential on cell surface [26]. The zeta potential of untreated HCC1833 cells and cells treated with ABT-263 (incubation periods t = 2, 6, 10 and 24 h) were measured and shown in Fig. 4. The zeta potential recorded characterizes the electrical double layer potential of the HCC1833 cells. Electrical characterization of cells is also dependent on the solvent composition of the suspension buffer, as shown in our previous work [17].

Zeta potential (ζ) of untreated cells (control population treated with DMSO only) was measured to be approximately about −6.34 mV. Control population measurement is an average measure at each incubation time point. At time t = 2 h post-treatment with ABT-263, HCC1833 cells showed increase in ζ by 1.79 mV, shifting from −6.34 mV to − 8.13 mV (shown as $\Delta\zeta_2$). Sudden increase in negative value of zeta potential post treatment with ABT-263 could be explained by the interaction of chloro-biphenyl and thio-phenyl moieties present in the drug [22]. At incubation time point t = 6 h post-treatment, a negative increase of 2.51 mV was observed from control population, consistent with apoptotic cascade of cells. Zeta potential at time t = 10 h showed steep increase in zeta potential to −10.20 mV with significant negative increase of 3.86 mV from control population. Significant change in zeta potential was observed for cells at 24 h incubation time period ($\Delta\zeta_{24}$) as ζ increased to −13.70 mV from −6.34 mV of control population. Change in zeta potential (7.36 mV) is indicated by Δζ with $^{*}P < 0.05$; $^{**}P < 0.01$; $^{***}P < 0.001$; n = 3 for each group.

The negative values of the zeta potential of cell membranes at physiological pH values are presumed to be caused by the presence of non-ionogenic groups within phospholipids, proteins and their polysaccharide conjugates [26]. Increase in negative values over incubation times post treatment of ABT-263 when compared to untreated control group corroborates expression of negatively charged phosphatidylserine (PS) carboxyl groups which are expressed during apoptosis. Redistribution of PS from the inner to the outer lipid layer of the plasmalemma contributes to the dramatic change in the zeta potential. The increase in zeta potential (Δζ) also indicates that lipids significantly contribute to the overall negative charge of the cell membrane. The results obtained also provided a feasibility study to understand change in electrical attributes of cell during apoptosis.

3.4. Dielectrophoretic response from cells

3.4.1. Cell collection measurements—Cell collection migration number (CCM) is the number of cells migrated and/or collected at the working and reference electrodes per minute due to repulsive or attractive forces experienced by the cells. Data indicating cell collection migration versus applied signal frequency for the DEP of untreated HCC1833 control cells and cells post treatment at incubation time points t = 2, 6, 10 and 24 h with ABT-263 are shown in Fig. 5. Cell collection number was observed and calculated for all time points at frequencies between 1 kHz and 100 MHz. The cell collection number of control population treated with DMSO was observed to be approximately 100 to 125 cells/min. This provides the baseline data for understanding electrokinetic behavior of viable cells handled under control (no drug treatment) conditions. Following ABT-263 treatment, CCM declined as a function of time.

Cells treated with 1 μM (clinically relevant concentration) of ABT-263 over incubation time points t = 2, 6, 10 and 24 h were tested using dielectrophoretic platform. Cell density per run was maintained at 1E + 3 cells/mL, with medium conductivity maintained between 5.5 to 7.5 mS/cm in the physiological range. Cells at time point t = 2 h post-treatment with ABT-263 showed increase in cell collection number from control population at frequencies lower than 1 MHz from 75 to 125 CCM. The majority of the sample population exhibited significantly higher cell collection number under this condition. This indicates sudden changes in the biochemical composition and ionic reorganization of cellular cytoplasm and cell membrane due to induction of apoptosis. At high frequencies, the cell collection number decreased indicating distinct cellular responses for early apoptotic cells at higher frequencies. As seen in Fig. 5a, cells collected after 6 h of treatment, stabilized over spectrum of frequency and significantly decreased from 75 to 25 CCM, relative to 2 h post treatment sample. This behavior indicates relatively less electrical activity within and outside of the cells, which correlates with the apoptotic cascade induced in cells. At higher frequencies, the cells migrating away from the electrode was observed to stabilize which indicates balances polarization behavior of cells under the application of gradient electric fields.

Similar trend was observed in cell collection number for time points t = 10 and 24 h, as shown in Fig. 5b. Cell collection number at these time points significantly dropped by 50% and 80% of the total number of cells collected in the control population. After 24 h of ABT-263 treatment, the occurrence of stable low CCM, where majority of population showed persistent low CCM indicating increase in number of cells undergoing late stage apoptosis. Upon apoptosis, effective dielectrophoretic response of cells decreases due to decrease in membrane conductance, which is a quantitative measure that indicates flow of ion species through ion channels across cell membrane. HCC1833 cells exhibited negative dielectrophoretic response at lower signal frequencies (f < 10 kHz) and a positive response at higher signal frequencies (f > 1 MHz). This frequency band was studied based on the cell's computed Claussius-Mossotti (CM) factor response (theory explained in [14,17]). Real value of CM factor indicates directionality of the movement of cells under the applied non-uniform electric fields. Values < zero correspond to frequencies at which cells experience negative DEP and values > zero correspond to positive DEP by cells in a given suspension

buffer. In all cell populations at varying incubation time points *t*, cell collection was observed at frequencies $f > 1$ kHz; the force reduced (in most cases) when the frequency exceeded 1 MHz. Significant differences in the dielectrophoretic response for all cell sample population was observed at higher frequencies between 1 MHz and 10 MHz. The data correlates well with percentage of cells detected at late stage apoptosis using flow cytometry after 24 h treatment with ABT-263.

3.4.2. Membrane capacitance measurements—Table 1 shows a summary of cellular characteristics according to modeling of the data using single-shell model [21]. Data indicate slight increase in cytoplasmic conductivity and specific membrane capacitance of HCC1833 with increase in incubation time post-treatment with ABT-263. Factors including cytoplasmic conductivity (σ_{cyto}, ionic concentration) and specific membrane capacitance (C_{mem}, membrane morphology quantitation) were calculated to observe effect of ABT-263 on NSCLC HCC1833 cells. In this study, the best fit for post-treatment data was obtained by superimposing single-shell model for different time points t = 0.5 (viable cell population) and 2 h, to estimate dielectric properties of cells undergoing apoptosis. C_{mem} is an important factor in understanding exocytosis, endocytosis and stimulus secretion mechanism that vary with biochemical cell cycle. Conductivity is a measure of the ability to conduct an electric field while the permittivity is a measure of cytoplasm or cell membrane to transmit the electric field [18].

The control untreated cells (viable population, time t < 0.5 h of treatment with DMSO) exhibited a cytoplasmic conductivity of 0.8 S/m and specific membrane capacitance of 12.5 mF/m^2, reflecting original state of cell morphology. Accumulation of charges in the suspending medium in response to applied gradient electric fields does have significant effect of the charge concentration within the cells. Thereby affecting the charge transport across the membrane and through pores and ion channels thus reflecting on specific membrane capacitance of the cell [20]. It has been well established that during apoptosis, increase in cytoplasmic conductivity and specific membrane capacitance of cells were observed. This was further supported by the modelled data obtained for time point t = 6, 10 and 24 h post-treatment. The cell population at these time point showed a persistent increase in their cytoplasmic conductivity to 0.96 S/m and 0.98 S/m. Gradual increase in specific membrane capacitance to 15.6 mF/m^2 and 16 mF/m^2 was measured for time points after 6 h. These results show a steady increase in the ionic concentration of the cytoplasm following the drug induction relative to control untreated cells.

In addition to significant change in cell's dielectrophoretic response through apoptotic cell cycle, cell radii was measured at time point t = 0.5 and 6 h. Slight drop in the cell radius was observed. Untreated cell population had a mean radius of approximately 10 μm. The cell's radius dropped to approximately 8 μm after 6 h of exposure to ABT-263. Although this change in cell radii was not significantly high, the contraction in cell's radius potentially leads to crowding of ions in cell cytoplasm. As a result, cell cytoplasm volume decreases leading to significant change in σ_{cyto}. Cells at time point t = 24 h had the smallest cell radii of ~7 μm, amongst majority of the population, which were also found to have the highest cytoplasmic conductivity. Changes in C_{mem} provides direct and quantitative measure of cell membrane morphology as a function of apoptotic induction. Understanding C_{mem} for non-

small lung cancer cells allows for enhancement of differences in cellular modifications and response due to specific drug in study.

4. Conclusion

Differences in cytoplasmic conductivity and specific membrane capacitance of treated and untreated cell population with drug ABT-263 was explored to understand apoptotic cell cycle of HCC1833 cells. In this study, we have shown detection of early apoptosis through persistent elevation in cell's dielectric properties as early as 2 h post-treatment. We demonstrated that apoptotic cells in NSCLCs can be identified as early as 2 h post treatment with the drug ABT-263 using dielectrophoresis. The work can be extended to study more complex mechanisms of cell subpopulation to better understand treatment sensitivity. Our studies have shown significant differences in dielectrophoretic signature of apoptotic cells as phosphatidylserine (PS) is exposed on the extracellular surface when the cells were exposed to a potent Bcl-2 family inhibitor drug (ABT-263). Decrease in cell radii along with increase in membrane capacitance indicating structural and morphological changes in cells were observed. Increase in cytoplasmic conductivity was observed as a potential result of ion species concentration within the cells during apoptosis. Furthermore, the dielectrophoretic results are comparable with zeta potential measurements indicating increase in charge imbalance during apoptosis. The results were also compared with standard bench-top flow cytometry method and DEP was found more powerful in capturing the early apoptotic cycle in cells. We conclude that DEP was capable of detecting apoptotic cell changes as early as 2 h as opposed to flow cytometry measurements, which showed significance in detection only after 24 h of treatment. This biophysical method of identifying the onset of apoptosis through non-invasive mechanism can potentially be used in conjunction with the standard benchtop methods with the advent of "precision medicine for cancer with next-generation functional diagnostics" that use the induction of apoptosis pathways in human cancer biopsy specimens to select therapy for individual patients, we think that our biophysical methods be of potential clinical application [27,28].

Acknowledgments

This work was funded by Cecil and Ida Green Endowment in Systems Biology at University of Texas at Dallas and grant funded by Lung Cancer SPORE P50CA70907. We thank Dr. Nesreen Alsmadi and Christopher Lewis from Schmidtke Laboratory at UT Dallas for their valuable inputs in flow cytometry data collection and analysis. We also thank Dr. Bryan Black from Neuronal Networks and Interfaces Laboratory at UT Dallas for his help with confocal microscope image acquisition and analysis.

References

1. Elmore S. Apoptosis: a review of programmed cell death. Toxicol Pathol. 2007; 35(4):495–516. [PubMed: 17562483]
2. Kuan N-K, Passaro E Jr. Apoptosis: programmed cell death. Arch Surg. 1998; 133(7):773–775. [PubMed: 9688008]
3. Barzegar E, et al. Effects of berberine on proliferation, cell cycle distribution and apoptosis of human breast cancer T47D and MCF7 cell lines. Iran J Basic Med Sci. 2015; 18(4):334. [PubMed: 26019795]
4. Tsuruo T, et al. Molecular targeting therapy of cancer: drug resistance, apoptosis and survival signal. Cancer Sci. 2003; 94(1):15–21. [PubMed: 12708468]

5. Ashkenazi A. Targeting the extrinsic apoptotic pathway in cancer: lessons learned and future directions. J Clin Investig. 2015; 125(2):487. [PubMed: 25642709]
6. Hankins HM, et al. Role of flippases, scramblases and transfer proteins in phosphatidylserine subcellular distribution. Traffic. 2015; 16(1):35–47. [PubMed: 25284293]
7. Collins JA, et al. Major DNA fragmentation is a late event in apoptosis. J Histochem Cytochem. 1997; 45(7):923–934. [PubMed: 9212818]
8. Riccardi C, Nicoletti I. Analysis of apoptosis by propidium iodide staining and flow cytometry. Nat Protoc. 2006; 1(3):1458–1461. [PubMed: 17406435]
9. Vermes I, et al. A novel assay for apoptosis flow cytometric detection of phosphatidylserine expression on early apoptotic cells using fluorescein labelled annexin V. J Immunol Methods. 1995; 184(1):39–51. [PubMed: 7622868]
10. Cheung K, Gawad S, Renaud P. Impedance spectroscopy flow cytometry: on-chip label-free cell differentiation. Cytometry A. 2005; 65(2):124–132. [PubMed: 15825181]
11. Chin S, et al. Rapid assessment of early biophysical changes in K562 cells during apoptosis determined using dielectrophoresis. Int J Nanomedicine. 2006; 1(3):333. [PubMed: 17717973]
12. Mulhall H, et al. Apoptosis progression studied using parallel dielectrophoresis electrophysiological analysis and flow cytometry. Integr Biol. 2015; 7(11):1396–1401.
13. Gascoyne PR, et al. Dielectrophoretic separation of cancer cells from blood. IEEE Trans Ind Appl. 1997; 33(3):670–678. [PubMed: 20011619]
14. Pethig R. Dielectrophoresis: using inhomogeneous AC electrical fields to separate and manipulate cells. Crit Rev Biotechnol. 1996; 16(4):331–348.
15. Menachery A, et al. Dielectrophoretic characterization and separation of metastatic variants of small cell lung cancer cells. UNE. 2016; 13:15.
16. Markx GH, Pethig R. Dielectrophoretic separation of cells: continuous separation. Biotechnol Bioeng. 1995; 45(4):337–343. [PubMed: 18623187]
17. Kumar RTK, IMG, Kinnamon D, Rodrigues DC, Prasad S. Use of dicationic ionic liquids as a novel liquid platform for dielectrophoretic cell manipulation. RSC Adv. 2016
18. Ismail A, et al. Characterization of human skeletal stem and bone cell populations using dielectrophoresis. J Tissue Eng Regen Med. 2015; 9(2):162–168. [PubMed: 23225773]
19. Augustyn A, et al. ASCL1 is a lineage oncogene providing therapeutic targets for high-grade neuroendocrine lung cancers. Proc Natl Acad Sci. 2014; 111(41):14788–14793. [PubMed: 25267614]
20. Labeed FH, Coley HM, Hughes MP. Differences in the biophysical properties of membrane and cytoplasm of apoptotic cells revealed using dielectrophoresis. Biochim Biophys Acta Gen Subj. 2006; 1760(6):922–929.
21. Broche LM, Labeed FH, Hughes MP. Extraction of dielectric properties of multiple populations from dielectrophoretic collection spectrum data. Phys Med Biol. 2005; 50(10):2267. [PubMed: 15876666]
22. Vogler M, et al. Bcl-2 inhibitors: small molecules with a big impact on cancer therapy. Cell Death Differ. 2009; 16(3):360–367. [PubMed: 18806758]
23. Knaapen M, et al. Cleaved PARP as a marker for apoptosis in tissue sections. Promega Notes. 1999; 72:7–9.
24. Fadok VA, et al. A receptor for phosphatidylserine-specific clearance of apoptotic cells. Nature. 2000; 405(6782):85–90. [PubMed: 10811223]
25. Zwaal RF, Schroit AJ. Pathophysiologic implications of membrane phospholipid asymmetry in blood cells. Blood. 1997; 89(4):1121–1132. [PubMed: 9028933]
26. Bondar OV, et al. Monitoring of the zeta potential of human cells upon reduction in their viability and interaction with polymers. Acta Nat (англоязычная версия). 2012; 4(1) (12).
27. Montero J, et al. Drug-induced death signaling strategy rapidly predicts cancer response to chemotherapy. Cell. 2015; 160(5):977–989. [PubMed: 25723171]
28. Friedman AA, et al. Precision medicine for cancer with next-generation functional diagnostics. Nat Rev Cancer. 2015; 15(12):747–756. [PubMed: 26536825]

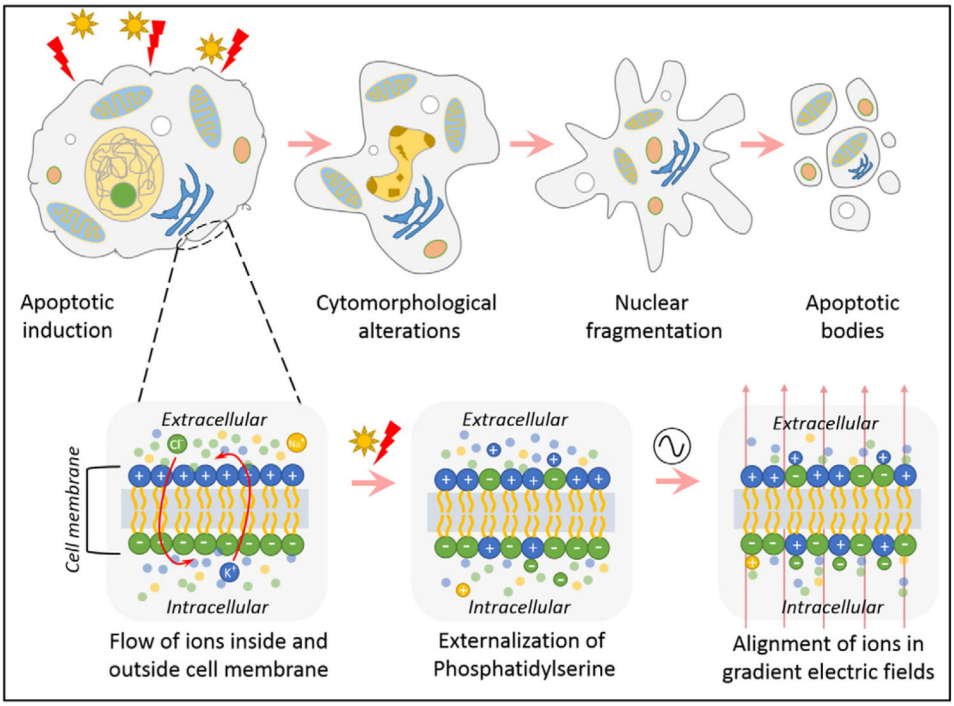

Fig. 1.

Illustration of an apoptotic cell cycle undergoing physiological cascade of events and electrical changes that happen simultaneously within and outside of the cell during apoptosis.

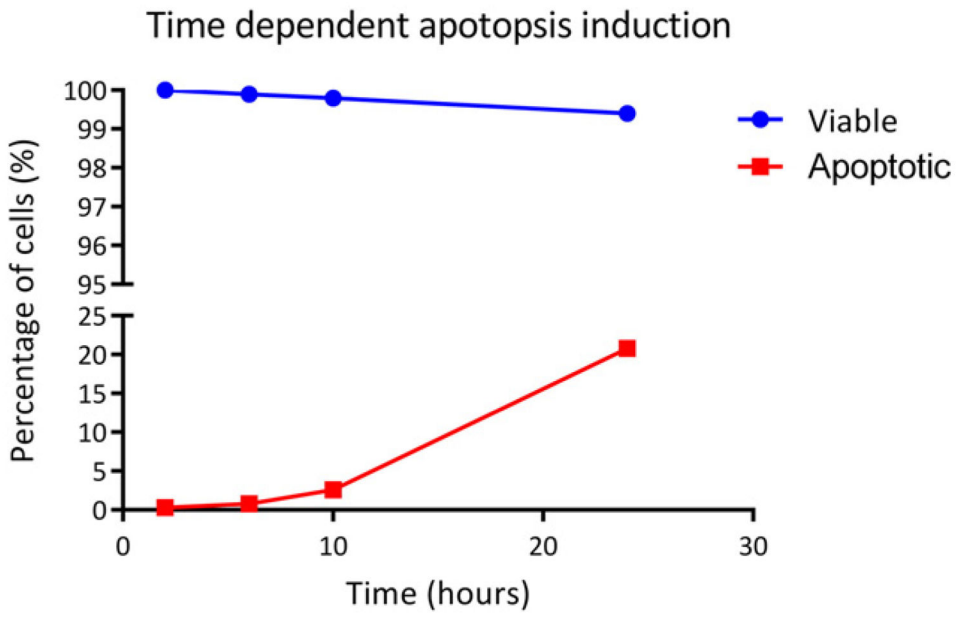

Fig. 2.

The percentage of viable and apoptotic populations after incubation period t = 2, 6, 10 and 24 h with BCL2 inhibitor ABT-263, as measured using flow cytometry by double staining cell sample by Annexin V-FITC and propidium iodide. Viable population was treated with DMSO for control studies.

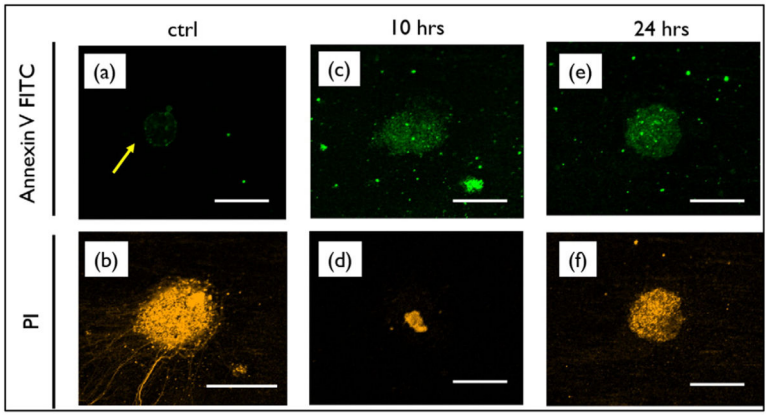

Fig. 3.

Microscopic evidence of apoptosis induction in HCC1833 cells double stained with Annexin V-FITC and PI dye, showing increase in early-mid stage apoptotic population [PI(−)/AnV(+)] and late stage apoptosis [PI(+)/AnV(+)] over 10 and 24 h incubation post-treatment with ABT-263. Control population image indicate AnV expression for cells treated with (a) DMSO only, (b) true positive of complete cell death [PI(+)]. Scale bar in the figure represents 5 μm.

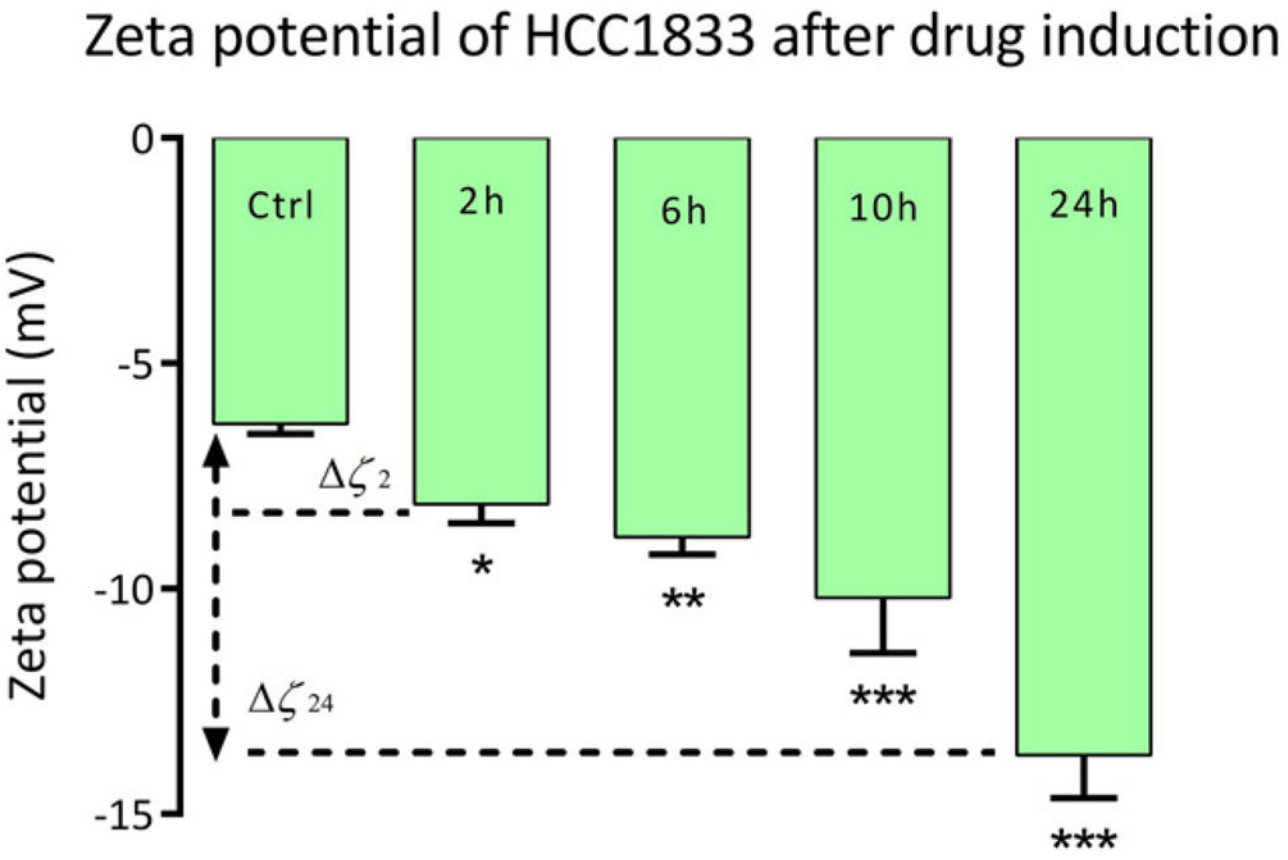

Fig. 4.

The zeta potential of HCC1833 before and after treatment with incubation time points t = 2 h, 6 h, 10 and 24 h. Control group indicates cell population with DMSO only. ($\Delta\zeta_{24}$) — shift of the zeta potential after 24 h of treatment with BCL2 inhibitor ABT-263; $^{*}P < 0.05$; $^{**}P < 0.01$; $^{***}P < 0.001$; n = 3 for each group.

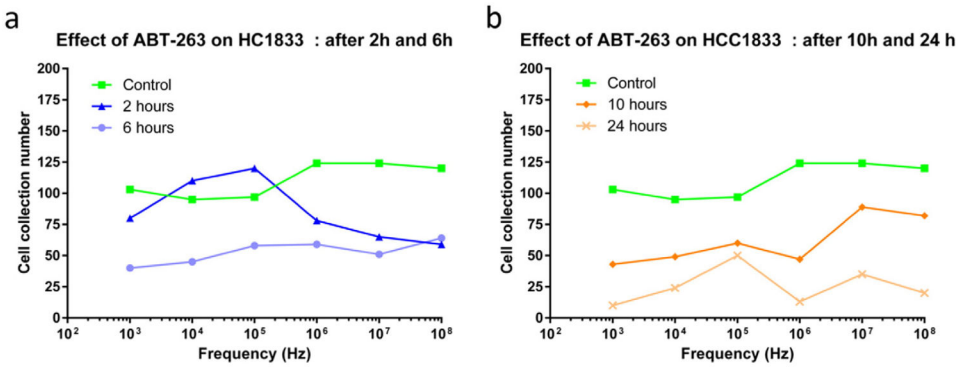

Fig. 5.

Average dielectrophoretic collection spectra indicating number of cells collected over a spectrum of applied signal frequency, for 3 experiments per condition. Effect of BCL2 inhibitor ABT-263 on NE-NSCLC cells HCC1833 after (a) time t = 2 and 6 h and (b) time t = 10 and 24 h with respect to control population treated with DMSO only. Data represented is an average of results obtained from n = 3 replicates per condition with covariance less than 5%.

Table 1

Electrophysiological data of HCC1833 cells before and after treatment with BCL2 inhibitor ABT-263, derived using single-shell model and dielectrophoretic data. Specific membrane capacitance for control cell population (DMSO) was observed to be within similar range for all time points.

Population	Incubation time (hours)	Cell radii (μm)	Cytoplasmic conductivity σ_{cyto} (S/m)	Specific membrane capacitance C_{mem} (mF/m^2)
Viable (DMSO)	0.5	10.0	0.80	12.5
Apoptotic (ABT-263)	6	8.0	0.96	15.6
	10	7.3	0.98	16.0
	24	7.0	0.98	16.0